# The Shell Model and Interatomic Potentials for Ceramics

Marshall Stoneham, John Harding, and Tony Harker

## Introduction

In a classification of solids according to their bonding character (into metals, ceramics and glasses, polymers, and semiconductors), the ceramic class includes an enormous range of industrially important materials. From the archetypal ionic solids through oxides to silicates, and to covalently bonded materials such as SiC, they exhibit a rich variety of structures and properties. They occur as structural materials, either on their own or as composites such as $SiC/Al_2O_3$. They are important functional materials, such as fast-ion conductors as electrolytes in fuel cells (for example $ZrO_2/Y_2O_3$ for hydrogen combustion) or batteries ($\beta$-alumina in the sodium-sulfur battery), ferroelectric materials such as $BaTiO_3$ and piezoelectrics such as PZT—a solid solution of $PbTiO_3$ and $PbZrO_3$. The high-temperature superconductors (for example, $YBa_2Cu_3O_7$) are ceramics above the superconducting transition temperature. The products of corrosion and oxidation are ionic materials, and the properties of oxide coatings are vital to the survival of high-temperature alloys in gas turbines or fuel-element claddings in nuclear reactors.

To understand the behavior of ceramic materials, and to optimize their production, processing, and application, it is often necessary to model their behavior at an atomic level. In some cases this is obvious. Ionic diffusion in a solid electrolyte is a self-evidently atomic process. In other cases the need for atomistic simulation is less clear. Oxidation, for example, is a subtle blend of atomic diffusion (often along grain boundaries), metal-ceramic bonding, stress relief, and grain growth. The course of oxidation can be spectacularly affected by impurities and alloying, and this can only be understood by considering the atomic-scale processes involved.

What then is a ceramic? Those we consider here are materials that, to a first approximation, may be treated as an assembly of non-overlapping spherical ions, held together by Coulomb attraction. We thus exclude covalent materials such as SiC and also materials such as intermetallics, which may take up crystal structures normally regarded as characteristic of ionic bonding. Electron-density maps, showing near-spherical charge densities, are often cited as evidence in favor of the ionic picture, but they can be misleading as they are dominated by the high electron densities near the nuclei, and there is no unique way of drawing the outlines of the ionic spheres. For the same reason, electron-density maps do not offer a resolution of the confused matter of ionic charge or ionicity. Although a direct definition of ionic charge could in principle be made in terms of the integrated electron density within an ionic volume, the choice of volume would always involve some arbitrary decisions. In general, one should use full formal charges (+1 for sodium, −1 for chlorine, in units of the electron charge $|e|$). An ion such as oxygen presents a problem. The $O^{2-}$ ion is not bound in free space, and so some would argue that it is unreasonable to give it a formal charge of −2. In the crystal, however, the ion is stabilized by the electrostatic potential of the neighboring positive ions. We shall return to the question of ionic charges, and to the oxide ion, later.

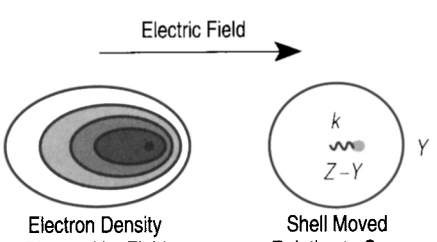


*Figure 1. The shell model of ionic polarizability compared with the distortion of electron density.*

To use this basic model for simulations, it is necessary to describe the interactions between the ions. In principle, it may be shown that the total energy of a crystal made up of $N$ ions at lattice spacing $R$ may be written as a sum of one-body, two-body, and higher order interactions:

$$E(R) = \sum_{i=1}^{N} E_i(R) + \sum_{i<j}^{N} \phi(R_{ij}) + \sum_{i<j<k}^{N} \phi^{(3)}(R_{ij}, R_{jk}, R_{ki}) \ldots \quad (1)$$

However, this formal expression gives no guidance on the order to which the sum must be taken or on the functional forms of the potentials. This is the point at which some physical insight is required.

## The Shell Model

The dominant term in the crystal energy is the Coulomb term arising from the interaction of the formal charges, which accounts for more than 80% of the cohesive energy. This attraction is countered by a short-range repulsion, arising from the exclusion principle, as ionic-charge densities overlap. Small additional contributions come from dispersion (van der Waals) interactions. Such a model, however, is incomplete. This is clear when one considers the dielectric response of the crystal, and dielectric polarization is a major term in the energies of defects. At low frequencies, one can explain the dielectric properties in terms of opposite movements of the ions in the electric field, producing local dipole moments: With formal ionic charge $Z$, if the ions are displaced from their equilibrium positions by $u_+$ and $u_-$, and if the vol-

ume occupied by a pair of ions is $\Omega$, then the polarization produced in a diatomic crystal will be $P = Zle|(u_+ - u_-)/\Omega$. At high frequencies, however, the ions are too massive to respond to the field, yet the dielectric constant is not unity. This is because the ions are themselves polarizable.

The simple introduction of ionic polarizability is not, however, enough, and it is worth describing in some detail why not, as this also has a bearing on the question of effective charges. The key quantities in the argument are the high- and low-frequency dielectric constants $\varepsilon(\infty)$ and $\varepsilon(0)$, and the longitudinal and transverse frequencies of long-wavelength lattice vibrations $\omega_L$ and $\omega_T$. Detailed derivations are given in most solid-state physics texts, and we merely quote the results here. For a point-ion model in which the ions do not polarize, one finds $\varepsilon(\infty) = 1$ and

$$\varepsilon(0) - \varepsilon(\infty) = (Ze)^2 / (\Omega\varepsilon_0 m\omega_T{}^2) \qquad (2)$$

where $m$ is a reduced ionic mass. For KBr, Cochran[1] shows that the right-hand side of this equation is 1.86, whereas $\varepsilon(0)$ is 4.46—a poor agreement. When ionic polarizability is introduced, a more realistic high-frequency dielectric constant results and

$$\varepsilon(0) - \varepsilon(\infty) = (\varepsilon(\infty) + 2)^2(Ze)^2/9\Omega\varepsilon_0 m\omega_T{}^2. \qquad (3)$$

However, substituting experimental values shows a discrepancy between 2.10 on the left and 3.92 on the right. It is tempting to introduce a polarization charge by reducing $Z$ to about 0.73 to resolve the discrepancy, but this will not be enough to make the calculated phonon-dispersion curves agree with experiment.

A more elegant solution is provided by the shell model, introduced by Dick and Overhauser[2] in 1958. Here the polarizability of the ions is included by representing each ion as a massive core and a massless shell of charge $Yle|$, the sum of the shell and core charges being $Zle|$. The core and shell are bound together by a harmonic potential (a "spring") with force constant $k$, giving a free-ion polarizability $(Ye)^2/k\varepsilon_0$. There is no need to restrict the core-shell interaction to be harmonic, and studies of induced-dipole moments[3] show disagreements between *ab initio* and shell-model predictions that an anharmonic spring might correct. The key to the success of the model, however, is to arrange for the short-range interactions between ions to be between the *shells*. If, to a first approximation, this short-range interaction is also harmonic with force constant $\kappa$, then when an ion is displaced it does not do so as a rigid unit but shifts the core more than the shell, giving a dipole moment $(Z - Y)u_{core} + Yu_{shell}$, with $u_{shell} = (k/(k + \kappa))u_{core} < u_{core}$. Thus the effective charge of the ion, deduced from the dipole moment it produces when it is displaced, is reduced to $Z(1 - (Y/Z)\kappa/(k + \kappa))$. This is but one example of the variety of effective charges that may be defined. (A wider survey is given by Catlow and Stoneham.[4]) The significant point is that a single charge

**Table I. Illustration of the Effect of Ionic Polarizability on Defect Energies and Distortions.**

| Case | Defect Energy (eV) | Nearest-Neighbor Position | Second-Neighbor Position |
|---|---|---|---|
| KCl:$Li^+$ | (−0.66) | | |
| Full model | −1.06 | (0.896, 0, 0) | (0.984, 0.984, 0) |
| No polarizability | −1.02 | (0.910, 0, 0) | (0.984, 0.984, 0) |
| KCl:$K^0$ | (8.08) | | |
| Full model | 5.07 | (1.092, 0, 0) | (0.976, 0.976, 0) |
| No polarizability | 5.35 | (1.105, 0, 0) | (0.978, 0.978, 0) |

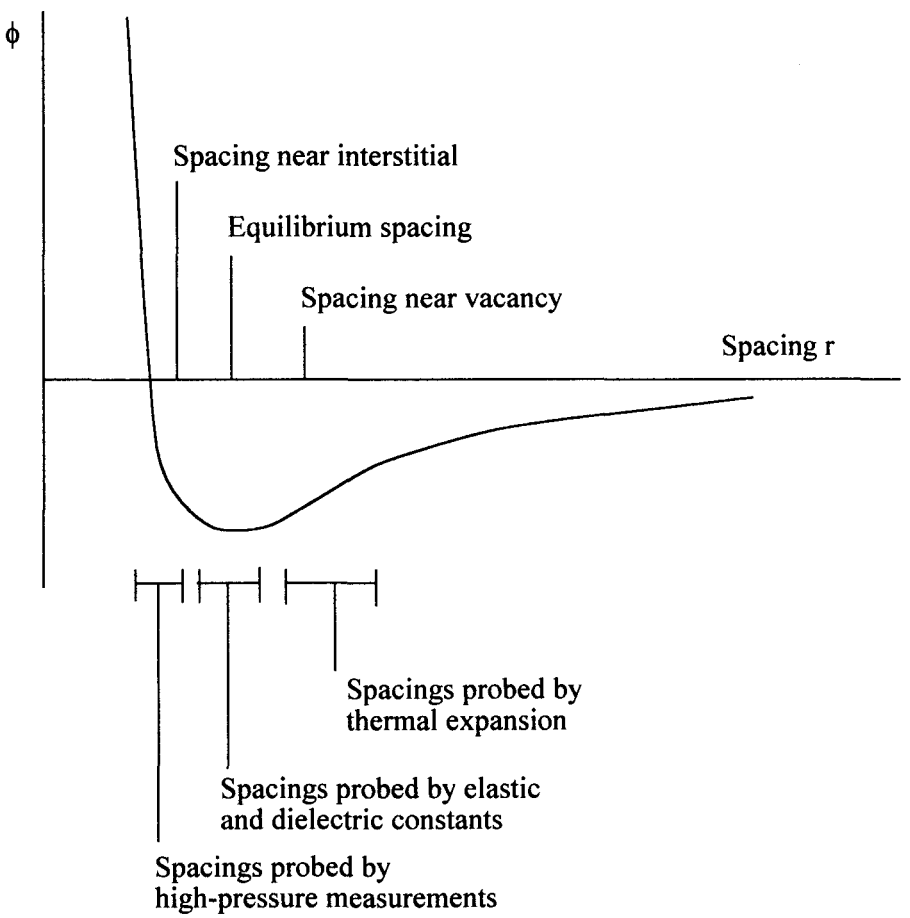


*Figure 2. A schematic, interionic, short-range potential function, showing the problems inherent in inferring the function across the significant range of distances from equilibrium properties alone.*

that defines the binding energy may differ from that which describes dielectric response. Clearly then, suitable choices of $Y$ and $\kappa$ can produce effective charges that will make Equation 3 hold. Further, the shell model produces excellent agreement throughout the phonon-dispersion diagram. The reason for this success is the interaction of the polarizability and the short-range repulsion. It is by no means the only such model that can be derived, and its popularity owes much to its physical picture (Figure 1) of the interactions, with the electronic polarization produced by the distortion of the ion's outer electrons mirrored in the motion of the shell relative to the core. The shell model can, however, represent any harmonic dipole approximation.

Why have we placed so much emphasis on the dielectric response of the crystal? The answer to this question lies in the coupling of polarization and distortion. In any defect problem, one may have elastic misfit (for example, the substitution of a $Cu^+$ ion by a much larger $Ag^+$) or misfit and a change of charge ($Li^+$ substituting for $Mg^{2+}$ in MgO). In order to evaluate the defect energy, it is important to include both the elastic response and the electrostatic polarization correctly. Here, incidentally, one sees the difficulties inherent in any model of the crystal that uses "non-ideal" charges: In the $Li^+ \rightarrow Mg^{2+}$ substitution there has been a real change of charge at the defect site of $-1|e|$. How is one to handle this situation if one treats the MgO as $Mg^{+1.8}O^{-1.8}$, typical charges deduced from some electronic-structure calculations?

Close to a defect, distortions are likely to be too large for a linear treatment of the response of the crystal to be adequate. (The interatomic distances involved can be very different from the equilibrium distances on which the coefficients of linear elasticity are based. This is also important, as will be discussed, in attempting to derive interatomic potentials.) There is no alternative in this region to treating the displacements and polarizations of the atoms in an explicit manner, finding the minimum energy configuration by varying the positions of the cores and shells. At long distances, both the elastic displacements **u** and the dielectric polarization **P** fall away as the inverse square of the distance $r$ from the defect. The elastic strain **e** falls off as $1/r^3$. The associated energies, therefore, which vary as the squares of **P** and **e**, when weighted by the associated volume elements decay as $1/r^4$ (elastic) and $1/r^2$ (polarization). Convergence with distance is therefore assured but is sufficiently slow that it is not possible to extend the explicit sum over ions over a sufficiently large region to include all the significant distortions. In practical calculations, the explicit region is joined at long range to a linear response region. Details of the methods may be found elsewhere.[5]

The effect of the coupling between polarization and distortion is illustrated in Table I. Here the energy to form defects in KCl is shown for two cases. In one case, a normal shell model is used. In the other case, ionic polarization is set to zero (though polarization through ion motion is included in full). The defects are $Li^+$ substituting for $K^+$, with a size mismatch but no change in charge, and $K^0$ substituting for $K^+$, with all the short-range parts of the potential unaltered so as to produce a change of charge but no change in ion size. The energies in brackets are those to form the defect in the undistorted crystal. The ionic polarizability makes a difference of 10% in the relaxation energy, both for the size-mismatch and charge-mismatch cases.

## Deriving Potentials

Armed with an understanding of the effects that must be included in an interionic potential, we need a scheme for deriving an explicit form. Broadly speaking, there are two approaches—empirical or theoretical. The empirical approach is to take an assumed function for the short-range potential, such as the Born-Mayer form $\phi_{AB}(r) = A_{AB}\exp(-r/\rho_{AB}) - C_{AB}/r^6$, with the parameters $A_{AB}$, $\rho_{AB}$, and $C_{AB}$ being characteristic of the ionic species A and B involved, and to determine these parameters and $Y$ and $\kappa$ of the shell model by fitting to experimental values of lattice parameter, elastic and dielectric constants, and possibly phonon frequencies or piezoelectric constants. The problem of this approach is demonstrated in Figure 2. Normal elastic and dielectric data involve small displacements from equilibrium, and a good fit to such data will not involve any information from the ranges of interatomic spacings that are found in defects. The situation is improved at short ranges by data from high-pressure shock waves or other high-pressure studies, and at longer ranges by thermal-expansion data. However, for many materials, even reliable elastic and dielectric measurements are not available, and the supplementary measurements are even more scarce. Furthermore, this only addresses the matter of intrinsic defects. If, for example, $Cl^-$ is substituted for $F^-$ in $CuF_2$, how are the $Cu^+$–$Cl^-$ and $F^-$–$Cl^-$ potentials to be found? For the former, a potential for $CuCl_2$ could be used, but the range of interatomic distances would not be appropriate. For the latter, one would probably be driven to intuitive schemes such as the geometric-mean assumption that $\phi_{AB}(r) = \sqrt{\phi_{AC}(r)\phi_{CB}(r)}$.

These limitations of empirical potentials turn one toward theoretical calculations of interactions. Two classes of approach are possible, based on first-principles calculations of the properties of atom clusters or on pairwise interactions. The former are in principle to be preferred, in that they would allow the terms beyond the pair interactions in Equation 1 to be determined. In practice this approach has not been widely adopted. Both computational convenience and ease of interpretation have favored the pairwise approach, in which the energy of interaction of two ions is computed directly. We will not discuss here the details of such calculations or of the relative merits of electron-gas and Dirac-Fock methods for evaluating the energy. (Comprehensive reviews are given by Wood and Pyper[6] and Pyper.[7]) There are, however, several points of principle that are worth stressing. The first requirement is that ions must be "prepared" in the configurations that they will adopt in the relevant crystal sites. For cations, the difference between a free-space ion such as $Na^+$ and the ion in a crystal is negligible, but anions with their more diffuse valence-electron densities will be compressed by the combination of the electrostatic potential well in which they reside and the repulsive effect of the core orbitals of their cation neighbors. (We refer to this combination as the site potential.) This compression is at its most extreme in the case of the $O^{2-}$ ion, which is only held together as a stable ion by these potentials. Second, it is assumed that the effect of any distortions that the ions may undergo is entirely represented by modifying the site potential. In this respect the calculation is not self-consistent. Third, the interaction energy is computed for uniform compression and expansion of the crystal so that the site symmetries are not altered. This ensures that only the short-range potential is sampled; self-consistent calculations on diatomic molecular ions are hard to interpret in terms of interionic potentials because of the necessity to subtract the ionic polarization from the energy. Finally, the dispersion energy may be evaluated: The van der Waals $1/r^6$ term is the first in a series usually written as $\phi_{AB}^{disp} = -\Sigma_{n=3}^{\infty} C_{AB}^{(2n)} r^{-2n}$.

The coefficients $C_{AB}^{(2n)}$ be computed, by a combination of first-principles calculations of ionic polarizabilities, approximation through the Slater-Kirkwood formula, interpolation, and extrapolation to higher $n$ by the Starkschall-Gordon formula. The details are given by Pyper,[8] who also reminds us that the expansion is only asymptotically correct and that each term should be modified by a function $f_n(r)$ to account for the overlap of the ions.

The term $E_i(R)$ in Equation 1 deserves further comment. In the context of pairwise ionic interactions, this represents the "rearrangement energy," which is the energy necessary to convert the free-space ion into the crystal ion. The discussion of the oxide ion by Harding and Pyper[9] has shown how this rearrangement energy is well-described by an expression dependent on the distance to the ion's nearest neighbors of the form $E_{re}(r) = E_0 + A_{re}\exp(-r/\rho_{re})$. As the values of $\rho_{re}$ are similar to the values of $\rho$ in empirically determined Born-Mayer potentials, for most purposes this rearrangement energy may be incorporated into the pair potential.

We have argued that theoretical potentials are more reliable than empirical ones, especially where distortions are large. An example is in the ordering of the energies of the surfaces of alumina, which have been computed using empirical[10] and theoretical[11] potentials. Although the two schemes agree on the ordering of energies for the unrelaxed surfaces, namely {10$\bar{1}$2}, {10$\bar{1}$2}, {10$\bar{1}$1}, {0001}, and {10$\bar{1}$0}, after relaxation the theoretical potential has the {0001} with the lowest energy whereas the empirical potential keeps the {10$\bar{1}$2} lowest. The stabilization of the {0001} surface involves large relaxations, which probe regions of the potential in which the empirical potential fails. The electron gas is in agreement with experiment in making the {0001} surface the most stable.

A further example of the ability of potentials, originally derived for bulk properties, to describe surfaces is the excellent agreement between the measured and calculated surface phonon density of states.[12] Here the potentials are seen to give a correct description both of the vibrational spectra and of the surface relaxations that modify them. The accuracy of the shell model is exemplified by studies of $Li^+$ substituting for $K^+$ in KCl. The small size of the $Li^+$ means that it can reduce the energy of the system by moving away from the perfect lattice site along a ⟨111⟩ direction, polarizing its neighbors as it does so. The energies in-

**Table II. Comparison Between *Ab Initio* and Shell-Model Calculations of the Relaxations of Ions Near the Basal-Plane Surface of Alumina.**

| | *Ab Initio* Density Functional | *Ab Initio* Hartree-Fock | Shell Model |
|---|---|---|---|
| Aluminum | −86% | −49% | −59% |
| Oxygen | +3% | −5% | +2% |
| Aluminum | −54% | −8% | −49% |
| Aluminum | +25% | | +26% |
| Oxygen | | | |

The layers of atoms are specified in the left-hand column, reading down from the surface, and the remaining columns give the changes in spacing. The density-functional calculations are by I. Manassidis and M.J. Gillan, *J. Am. Ceram. Soc.* **77** (1994) p. 335, and the Hartree-Fock calculations are by J.D. Gale, C.R.A. Catlow, and W.C. Mackrodt, *Mod. Simul. Mater. Sci. Eng.* **1** (1992) p. 73.

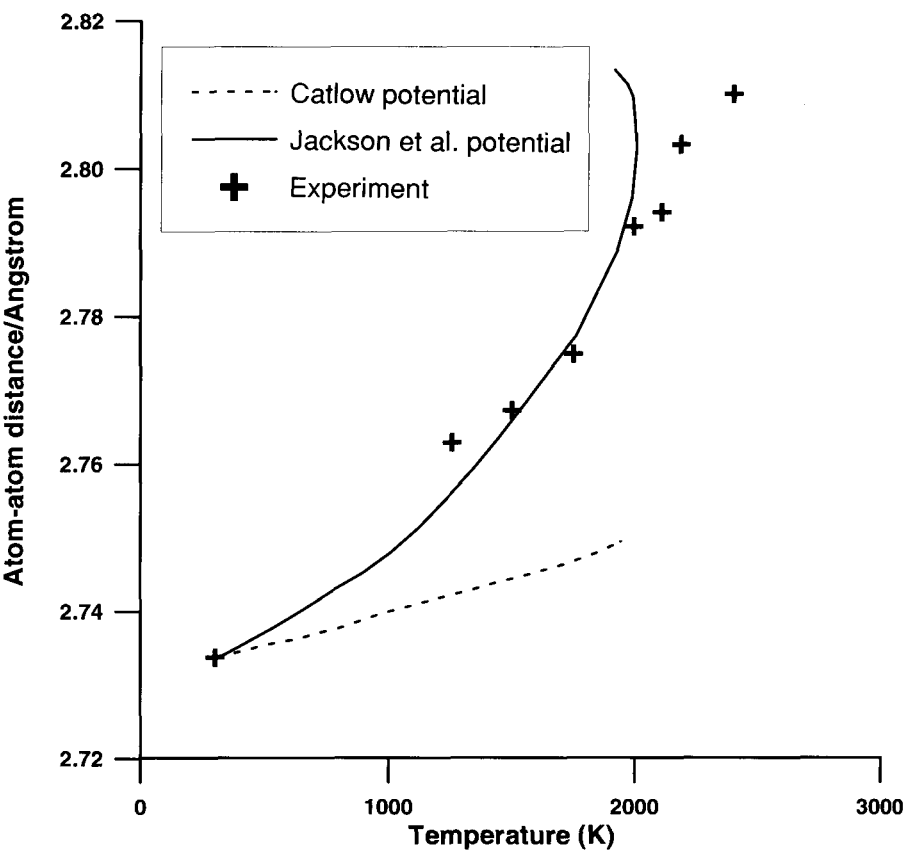


*Figure 3. Thermal expansion of urania predicted by an empirical potential based on equilibrium properties (C.R.A. Catlow,* Proc. R. Soc. A ***353*** *[1979] p. 533) and by one that also uses high-temperature data (R.A. Jackson, A.D. Murray, J.H. Harding, and C.R.A. Catlow,* Philos. Mag. A ***53*** *(1986) p. 27) compared with experiment (J.E. MacDonald, PhD dissertation (University of Oxford, 1985).*

volved are very small, but the occurrence of off-centering is correctly predicted by the model.

## Comparison With *Ab Initio* Results

Although the shell model has a long history of successful applications to a variety of problems, it is important to check the extent to which it remains a reasonable description of materials of lower ionicity or where distortions are large. An example is the basal plane of alumina, where distortions, as we already mentioned, are large and where the use of a fully ionic $Al_2^{3+}O_3^{2-}$ model could be questioned. This may be addressed by comparing the detailed predictions of electronic-structure calculations using density-functional theory or Hartree-Fock methods with those of potential models. Table II shows that the details of the relaxations are quite similar, and furthermore it is found that the material remains highly ionic in the surface region, with only a very small amount of valence charge on aluminum, reducing the charge slightly below 3+. The computed surface energy is 1.76 J $m^{-2}$ in the density-functional calculation, 2.03 J $m^{-2}$ with the shell model. Note that the Hartree-Fock calculation, in which the treatment of quantum-mechanical exchange is better than that of the local-density approach but correlation is neglected, gives a slightly larger unrelaxed surface energy than does the local-density calculation.

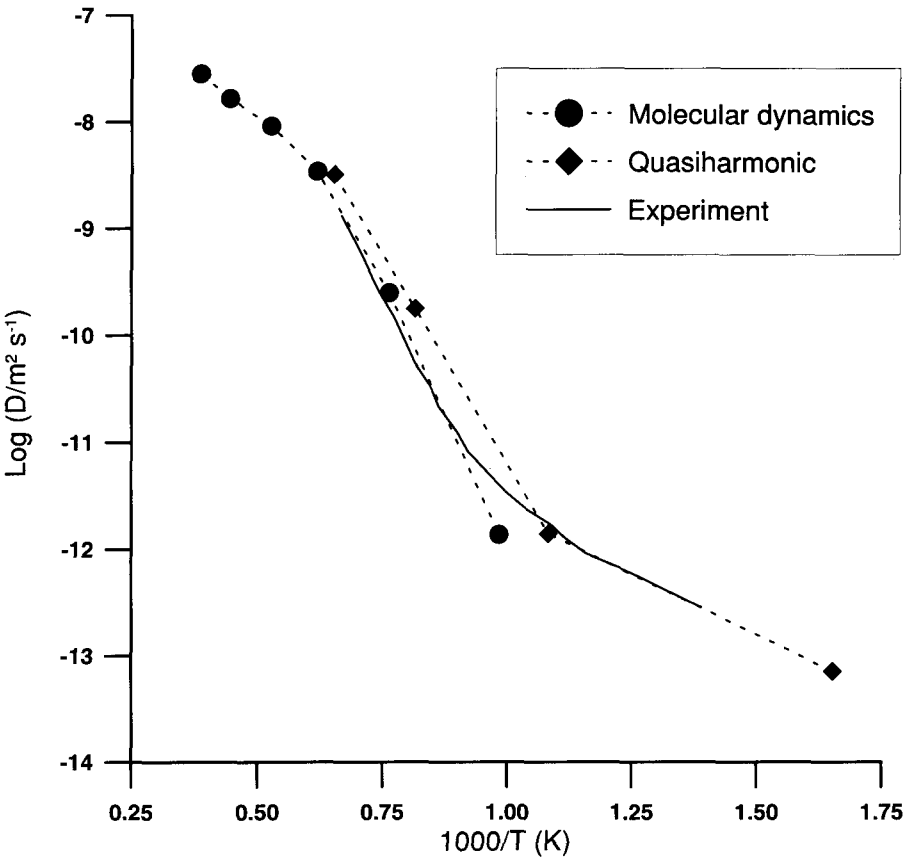


*Figure 4. The cation diffusion coefficient in lithia, computed using a shell model in a quasiharmonic model and using molecular dynamics (A.V. Chadwick, K.W. Flack, J.H. Strange, and J.H. Harding,* Solid State Ionics ***28–30*** *[1988] p. 185).*

## Applications

Here we aim to show the wide range of problems in perfect and defective materials, surfaces, and interfaces, to which the shell model has been successfully applied. We have already stated that the model describes extremely well the details of the phonon spectrum, that is, the harmonic region of the potential. Thermal expansion can also be modeled by these potentials, but as shown in Figure 3 for urania, a potential that is fitted only to equilibrium properties will fail where one that uses some high-temperature information succeeds.

Interionic potentials may be used both in static simulations and in molecular dynamics. A case in point is the computation of cation diffusion in lithia. In an idealized picture of diffusion, the ion must move from one lattice site to another over a potential barrier, the midpoint of the path being a saddle point on the potential-energy surface. The diffusion rate may be derived[13] from a quasiharmonic approximation to the atomic jump rate $\Gamma = A \exp(-E_A/k_BT)$, in which the rate factor is computed from vibrational frequencies at the lattice site and at the saddle point, and the activation energy is the difference in energy between the lattice site and the saddle point. Alternatively, in a molecular-dynamics simulation, the slope of the mean-square displacement of the ions at long times is proportional to the diffusion constant. Each technique has its advantages. At low temperatures, jumps are so infrequent that molecular-dynamics runs would have to be impractically long to observe diffusion. At high temperatures, the assumption of an otherwise perfect crystal makes the quasiharmonic model decreasingly plausible as the melting point is approached. By combining the two models, as shown in Figure 4, a wide temperature range can be covered. Agreement with experiment is good, and where results from both theoretical models are available, they agree with each other. Excellent agreement between models and experiment is also shown by study of intrinsic diffusion in MgO.[14]

The applications of atomistic models are not mere academic exercises. An excellent example of an industrial application is Harding's[15] analysis of the effect of dopants on the corrosion of zircaloy. Zircaloy-2 is a zirconium-based alloy used to clad fuel in nuclear reactors that use boiling water as the coolant. After long periods in the core, the fuel elements were found to exhibit nodular corrosion. Harding's work showed the correlation between the sites occupied by the impurities in their various charge states and the corrosion.

A significant example of the shell model succeeding in cases that might appear to be beyond its scope is for the $V^-$ center in MgO.[16] This is a site from which a $Mg^{2+}$ ion has been removed, attracting a single hole to produce a center with a net charge of $-1$ relative to the crystal. The hole is localized to change one neighboring $O^{2-}$ to an $O^-$. The shell model, as well as predicting correctly that the polarization energy is sufficient

to localize the hole, offers a very accurate description of the optical transitions caused by charge transfer, in which the hole moves to other neighbors.

## Extending the Model

The extension of the shell model to metal-ceramic interfaces relies on the fact that the energetics will be dominated by electrostatic interactions—in this case, those between ionic charges in the ceramic and the image charges in the metal, which are generated in order to make the metal surface an equipotential.[17] Modifications must be made to the simple picture to account for the fact that the metal cannot redistribute its electronic-charge density to form point image charges because the sharpness of the image is restricted by the Fermi wavelength. Furthermore, attempting to embed the ions of the ceramic in the free-electron sea of the metal introduces a repulsive energy because of the overlapping charge densities, and this repulsion helps to prevent the ions from collapsing into interstitial positions in the metal surface. In many respects the structures of metal-ceramic interfaces are still uncertain, but Table III shows that the shell-model predictions are similar to those of full electronic-structure calculations using the local-density approximation.

A common extension to the basic shell model is to add extra terms to model the angle-dependent forces that might be expected if there were some degree of covalency in the material. There is no universally accepted form for the term $\phi^{(3)}(R_{ij}, R_{jk}, R_{ki})$ in Equation 1. The one that is often used is proportional to the square of the deviation of the bond angle from the equilibrium angle. This form has an intuitive appeal in that it is harmonic. However, there is no guarantee that the functional form will still be correct at large distortions. Nevertheless, some kind of three-body correction is clearly necessary. The effect of adding a term such as this to a model for $\alpha$-quartz can be seen from Table IV.

Making models more elaborate, however, introduces additional parameters and raises the question of overfitting. One must ask whether the parameters that result in good agreement with experiment for the materials for which they are fitted will result in nonsense when applied outside that range. Some reassurance comes from a series of calculations in which potentials from the binary oxides MgO and $SiO_2$ were augmented with a three-body term fitted to the forsterite form of $Mg_2SiO_4$, and applied

**Table III. Comparison Between *Ab Initio* and Shell-Model Calculations of the Interfacial Energy and Dilations at an Interface Between Metallic Silver and MgO.**

| | Local-Density Approximation | | | | Shell Model | |
|---|---|---|---|---|---|---|
| | Schönberger et al. | | Li et al. | | Duffy et al. | |
| | *Energy (eV)* | *Dilation* | *Energy (eV)* | *Dilation* | *Energy (eV)* | *Dilation* |
| **Ag Over $O^{2-}$ Site** | −0.88 | | −0.3 | 1.28 | −0.32 | 1.20 |
| **Ag Over $Mg^{2+}$ Site** | −0.45 | 1.19 | | | −0.60 | 1.20 |
| **Ag Over Interstitial Site** | −0.58 | | | | −0.48 | 1.30 |

The different rows in the table are for different positions of the two crystals relative to each other. The *ab initio* calculations are by U. Schönberger, O.K. Anderson, and M. Methfesset, *Acta Metall.* **40** (1992) p. S1 and by C. Li, R. Wu, A.J. Freeman, and C.L. Fu, *Phys. Rev. B* **48** (1993) p. 8317. The shell-model results are from D.M. Duffy, J.H. Harding, and A.M. Stoneham, *J. Appl. Phys.* **76** (1994) p. 2791.

**Table IV. The Improvement in the Fitting of Experimental Data for $\alpha$-Quartz When a Three-Body Term Is Included in the Potential (C.R.A. Catlow, C.M. Freeman, M.S. Islam, R.A. Jackson, M. Leslie, and S.M. Tomlinson, *Philos. Mag. B* 58 [1988] p. 123).**

| Property | Experiment | Two-Body Potential | Three-Body Potential |
|---|---|---|---|
| $C_{11}$ | 8.683 | 6.204 | 8.815 |
| $C_{13}$ | 1.193 | 1.629 | 1.151 |
| $C_{14}$ | −1.8064 | −1.012 | −1.666 |
| $C_{33}$ | 10.498 | 7.466 | 10.605 |
| $C_{44}$ | 5.826 | 3.301 | 5.296 |
| $C_{66}$ | 3.987 | 2.737 | 4.269 |
| $\varepsilon_{11}(0)$ | 4.520 | 5.513 | 4.452 |
| $\varepsilon_{33}(0)$ | 4.460 | 6.086 | 4.812 |
| $\varepsilon(\infty)$ | 2.4 | 2.069 | 2.04 |

Elastic-constant values are in $10^{12}$ dynes/cm$^2$.

**Table V. The Transferability of a Shell-Model Potential, Including Three-Body Terms Among the Polymorphs of Magnesium Silicate as Calculated by G.D. Price, S.C. Parker, and M. Leslie, *Phys. Chem. Min.* 15 (1987) p. 181.**

| Property | Forsterite | | $\beta$-$Mg_2SiO_4$ | | Spinel | |
|---|---|---|---|---|---|---|
| | Experiment | Calculated | Experiment | Calculated | Experiment | Calculated |
| *a* (Å) | 4.754 | 4.784 | 5.698 | 5.654 | 8.065 | 8.020 |
| *b* (Å) | 10.194 | 10.261 | 11.438 | 11.397 | | |
| *c* (Å) | 5.981 | 5.991 | 8.257 | 8.281 | | |
| *K* (GPa) | 125 | 154 | 174 | 220 | 184 | 250 |
| $\mu$ (GPa) | 81 | 78 | 114 | 117 | 119 | 126 |

The quantities are the lattice parameters *a*, *b*, and *c* and the bulk *K* and shear $\mu$ moduli.

to other polymorphs of $Mg_2SiO_4$. Table V shows how successful this approach is and confirms the transferability of carefully parameterized potentials from one system to another. This table also shows that the shell model has great potential for modeling a wide range of materials of geological importance.

Other extensions to the basic shell model add aspects of electronic structure into the calculations. In general the assumption is made that it is possible simply to add correction terms to the shell-model results. Examples include the study of different charge states of ions in crystals where it is necessary to introduce ionization energies. These are often taken to be equal to the free-ion values. There exists a fairly recent review of the small-polaron theory, which is the basis of these approaches.[18] Another way in which electronic terms may be included as a *post hoc* correction is by computing a change in the crystal-field energy of an ion with a partly filled electronic shell as a result of the distortion of the surrounding crystal. Again, the assumption is that the spatial extents of the wave functions do not change with the distortion, so that the short-range potentials of the shell model and the crystal-field parameters of the electronic energy may be taken as constants.

## Summary

Calculations supplement experiment in several ways. With models it is possible to calculate effects one at a time, whereas experiments always present a mixture of effects. In complex materials or complex processes, disentangling which effects are present and which (if any) dominate is not a trivial process. Computer simulations can be controlled in ways that may be experimentally impracticable, and this is particularly important in understanding processes in materials. By studying the detailed behavior of models, it is possible to come up with new ideas that, on the one hand, can be used to criticize and correct analytical theories and on the other to suggest new experiments. Simulations can be used to model materials under conditions of temperature and pressure that may be inaccessible in the laboratory, and in this respect they are becoming a valuable tool for geophysicists.

This article has shown that the shell model is a reliable, predictive tool for a wide variety of problems in a wide variety of materials. It can be applied to materials that would conventionally be regarded as partly covalent, and with simple extensions even to silicates and similar compounds. The shell model describes bulk materials and surfaces with equal success, and forms the basis of a simple model of metal-ceramic interfaces. It may be applied in static and dynamic simulations. In fact, in any process in which the character of the bonding does not change so that the underlying picture of interacting ions with fixed charges holds, we expect the shell model to continue providing insight into problems of technical importance.

## References


1. W. Cochran, *The Dynamics of Atoms in Crystals*, edited by Edward Arnold (1973).
2. B.G. Dick and A.W. Overhauser, *Phys. Rev.* **112** (1958) p. 603.
3. M. Wilson and P.A. Madden, *J. Phys.: Conden. Matt.* **5** (1993) p. 2687.
4. C.R.A. Catlow and A.M. Stoneham, *J. Phys. C: Solid Phys.* **16** (1983) p. 4321.
5. C.R.A. Catlow and W.C. Mackrodt, eds., *Computer Simulation of Solids* (Springer-Verlag, 1982).
6. C.P. Wood and N.C. Pyper, *Chem. Phys. Lett.* **81** (1981) p. 395.
7. N.C. Pyper, *Philos. Trans. R. Soc. A* **320** (1986) p. 107.
8. N.C. Pyper, *Adv. Solid State Chem.* **2** (1991) p. 223.
9. J.H. Harding and N.C. Pyper, *Philos. Mag. Lett.* **71** (1995) p. 113.
10. N.L. Allen, D.L. Cooper, and W.C. Mackrodt, *Mol. Simul.* **4** (1990) p. 269.
11. C.R.A. Catlow, M. Dixon, and W.C. Mackrodt, in Reference 5, p. 130.
12. J.P. Hoare, P. Masri, and P.W. Tasker, AERE Report R10752 (1983).
13. G.H. Vineyard, *J. Phys. Chem. Solids* **3** (1957) p. 121.
14. M.H. Yang and C.P. Flynn, *Phys. Rev. Lett.* **73** (1994) p. 1809.
15. J.H. Harding, *J. Nucl. Mater.* **202** (1993) p. 216.
16. M.J. Norgett, A.P. Pathak, and A.M. Stoneham, *J. Phys. C: Solid State Phys.* **10** (1977) p. 555.
17. D.M. Duffy, J.H. Harding, and A.M. Stoneham, *Philos. Mag. A* **67** (1993) p. 865.
18. A.M. Stoneham, *J. Chem. Soc. Faraday Trans. II* **85** (1989) p. 505. □